



LJMU Research Online

Foulkes, JM, Deplanche, K, Sargent, F, Macaskie, LE and Lloyd, JR

A Novel Aerobic Mechanism for Reductive Palladium Biomineralization and Recovery by Escherichia coli

<http://researchonline.ljmu.ac.uk/id/eprint/3544/>

Article

Citation (please note it is advisable to refer to the publisher's version if you intend to cite from this work)

Foulkes, JM, Deplanche, K, Sargent, F, Macaskie, LE and Lloyd, JR (2016) A Novel Aerobic Mechanism for Reductive Palladium Biomineralization and Recovery by Escherichia coli. Geomicrobiology Journal, 33 (3-4). pp. 230-236. ISSN 1521-0529

LJMU has developed **LJMU Research Online** for users to access the research output of the University more effectively. Copyright © and Moral Rights for the papers on this site are retained by the individual authors and/or other copyright owners. Users may download and/or print one copy of any article(s) in LJMU Research Online to facilitate their private study or for non-commercial research. You may not engage in further distribution of the material or use it for any profit-making activities or any commercial gain.

The version presented here may differ from the published version or from the version of the record. Please see the repository URL above for details on accessing the published version and note that access may require a subscription.

For more information please contact researchonline@ljmu.ac.uk

<http://researchonline.ljmu.ac.uk/>



A novel aerobic mechanism for reductive palladium biomineralization and recovery by *Escherichia coli*

Journal:	<i>Geomicrobiology Journal</i>
Manuscript ID:	UGMB-2015-0116.R1
Manuscript Type:	Special Issue
Date Submitted by the Author:	n/a
Complete List of Authors:	Foulkes, Joanne; Liverpool John Moores University, Pharmacy and Biomolecular Science Deplanche, Kevin; University of Birmingham, School of Biosciences Sargent, Frank; University of Dundee, College of Life Sciences Macaskie, Lynne; University of Birmingham, School of Biosciences Lloyd, Jon; University of Manchester, School of Earth, Atmospheric and Environmental Sciences
Keywords:	biomineralization, metal reduction, bioremediation

SCHOLARONE™
Manuscripts

1
2
3 1 A novel aerobic mechanism for reductive palladium

4
5
6 2 biomineralization and recovery by *Escherichia coli*

7
8
9 3

10
11 4 JOANNE M. FOULKES^a, KEVIN DEPLANCHE^b, FRANK SARGENT^c, LYNNE E.

12
13 5 MACASKIE^b, JONATHAN R. LLOYD^{a*}

14
15
16 6

17
18 7 *a. Williamson Research Centre for Molecular Environmental Science and School of*

19
20 8 *Earth, Atmospheric and Environmental Sciences, University of Manchester, Oxford*

21
22 9 *Road, Manchester M13 9PL, UK*

23
24 10 *b. Unit of Functional Bionanomaterials, School of Biosciences, University of*

25
26 11 *Birmingham, Edgbaston, Birmingham B15 2TT, UK*

27
28 12 *c. Division of Molecular Microbiology, College of Life Sciences, University of*

29
30 13 *Dundee, Dundee DD1 5EH, UK*

31
32
33 14

34
35 15 *Corresponding author, Jon.Lloyd@manchester.ac.uk

36
37 16 Tel: (0161) 275 7155

38
39 17 Fax: (0161) 306 9361

40
41
42 18

43
44 19 Aerobically-grown *E. coli* cells reduced Pd(II) via a novel mechanism using formate

45
46 20 as the electron donor. This reduction was monitored in real-time using extended X-ray

47
48 21 absorption fine structure. Transmission electron microscopy analysis showed that

49
50 22 Pd(0) nanoparticles, confirmed by X-ray diffraction, were precipitated outside the

51
52 23 cells. The rate of Pd(II) reduction by *E. coli* mutants deficient in a range of

53
54 24 oxidoreductases was measured, suggesting a molybdoprotein-mediated mechanism,

55
56 25 distinct from the hydrogenase-mediated Pd(II) reduction previously described for

1
2
3 26 anaerobically-grown *E. coli* cultures. The potential implications for Pd(II) recovery
4
5 27 and bioPd catalyst fabrication are discussed.
6
7
8

9
10
11
12
13
14
15
16
17
18
19
20
21
22
23
24
25
26
27
28
29

30
31 **Keywords:** palladium nanoparticles, *Escherichia coli*, biomineralization.

32
33
34
35
36
37
38
39
40
41
42
43
44
45
46
47
48
49
50
51
52
53
54
55
56
57
58
59
60

31 Introduction

32 The microbial reduction of metals and radionuclides has attracted much interest, as it
33 can be potentially harnessed for bioremediation, metal recovery, the fabrication of
34 novel nanobiominerals and even energy generation in biobatteries (Lloyd 2003; Lloyd
35 et al. 2008; Lovley 2006;). For example, the sulfate-reducing bacterium (SRB)
36 *Desulfovibrio desulfuricans* has been shown to use a periplasmic hydrogenase
37 supplied with hydrogen to reduce soluble Pd(II), resulting in the precipitation of Pd(0)
38 nanoparticles in the periplasm of the cell ('bioPd'). However SRB produce H₂S, a
39 potent catalyst poison that must be removed before making the bioPd. Other
40 organisms capable of this metal bioreduction include the Gram-negative bacteria
41 *Shewanella oneidensis* (De Windt et al. 2005), *Escherichia coli* (Deplanche et al.
42 2010, 2014; Mabbett et al. 2006), *Pseudomonas putida*, *Cupriavidus necator* (Søbjerg
43 et al. 2009), *Cupriavidus metallidurans* (Gauthier et al. 2010), *Paracoccus*
44 *denitrificans* (Bunge et al. 2010), *Rhodobacter sphaeroides* (Redwood et al. 2008),
45 *Rhodobacter capsulatus* (Wood et al. 2010), and the Gram-positive bacteria *Bacillus*
46 *sphaericus* (Creamer et al. 2007), *Arthrobacter oxydans* (Deplanche et al. 2014;
47 Wood et al. 2010), *Micrococcus luteus* (Deplanche et al. 2014), *Staphylococcus sciuri*
48 (Søbjerg et al. 2009) and *Clostridium pasteurianum* (Chidambaram et al. 2010). This
49 property has allowed the use of 'palladised' whole cells or processed biomineral
50 directly in industrially important reactions, often showing superior activity compared

1
2
3 51 with a commercially available carbon-supported palladium catalyst. A number of
4
5 52 studies have investigated the catalytic activity of bioPd, demonstrating its use in
6
7 53 remediative reactions such as the reduction of Cr(VI) to Cr(III) (Beauregard et al.
8
9
10 54 2010; Mabbett et al. 2006), the dehalogenation of chlorophenol, polychlorinated
11
12 55 biphenyls, polybrominated diphenyl ethers (Baxter-Plant et al. 2003; De Windt et al.
13
14 56 2005; Harrad et al. 2007), trichloroethylene (Hennebel et al. 2009a, 2009b), and the
15
16 57 pesticide γ -hexachlorocyclohexane (Mertens et al. 2007), in 'greener' chemical
17
18 58 synthesis such as the hydrogenation of itaconic acid (Creamer et al. 2007) and 2-
19
20 59 pentyne (Bennett et al. 2010), in Heck and Suzuki reactions (Bennett et al. 2013;
21
22 60 Deplanche et al. 2014), and also in the application of bioPd as a fuel cell
23
24
25 61 electrocatalyst to produce electricity from hydrogen (Orozco et al. 2010; Yong et al.
26
27 62 2007). In each case where the bioPd was compared with an abiotically-produced
28
29 63 palladium catalyst (finely-divided or supported on a carbon matrix), the bioPd was
30
31 64 more active than or at least as active as the commercially available alternative.
32
33
34 65
35
36 66 Production of catalytically active bioPd also was reported by an aerobically-grown
37
38 67 *Serratia* sp. (Beauregard et al. 2010; Deplanche et al. 2014) under which condition
39
40 68 hydrogenases are not expressed. Also, cells of *E. coli* deficient in the three major
41
42 69 hydrogenases reduced Pd(II) (albeit slowly: Deplanche et al. 2010), and showed
43
44 70 larger Pd-nanoparticles located on the outer surface of the cells. This suggested an
45
46 71 alternative mechanism of Pd(II) reduction which has not been investigated.
47
48
49 72
50
51 73 *E. coli* produces bioPd which is comparably active to that produced by *D.*
52
53 74 *desulfuricans* (Deplanche et al. 2014). This also provides a very useful model
54
55 75 organism since it is facultatively anaerobic and has well-defined molecular tools to
56
57
58
59
60

1
2
3 76 elucidate reaction mechanisms under aerobic and anaerobic conditions. The enzymes
4
5 77 potentially involved in the bioreduction of palladium by *E. coli* under the latter
6
7 78 conditions are the nickel-dependent hydrogenase enzymes Hyd-1, Hyd-2, and Hyd-3,
8
9 79 and the formate dehydrogenase molybdoenzymes FDH-N, and FDH-H. Another
10
11 80 molybdoenzyme, FDH-O, is expressed under both aerobic and anaerobic conditions.
12
13 81 A possible role for FDH-O is to allow bacteria to adapt rapidly to a sudden shift from
14
15 82 aerobic respiration to anaerobiosis, before FDH-N has been produced in sufficient
16
17 83 amounts to continue formate metabolism (Abaibou et al. 1995). Hyd-1, Hyd-2, FDH-
18
19 84 O, and FDH-N are membrane-bound and periplasmically oriented, whereas Hyd-3
20
21 85 and FDH-H are subunits of the formate hydrogenlyase (FHL) complex, an
22
23 86 intracellular enzyme complex that is also membrane-bound but which faces into the
24
25 87 cytoplasm. The mechanisms responsible for the formate-dependent bioreduction by
26
27 88 anaerobically-grown cultures of *E. coli* have been studied, showing that the
28
29 89 hydrogenase enzymes Hyd-1 and Hyd-2 are mainly responsible for Pd(II)
30
31 90 bioreduction (Deplanche et al. 2010). In a study of formate-dependent Pd(II)
32
33 91 bioreduction by *Desulfovibrio fructosovorans*, the deletion of the periplasmic
34
35 92 hydrogenases caused the Pd(0) nanoparticles to be relocated to the cytoplasmic
36
37 93 membrane site of the remaining hydrogenases, indicating that the periplasmic
38
39 94 hydrogenases are at least partially involved (Mikheenko et al. 2008).
40
41
42
43
44
45 95
46
47 96 The growth yield of anaerobic cultures is lower than that of aerobic cultures, and for
48
49 97 economic production at scale a method of growth of high biomass density is required.
50
51 98 When using anaerobic cultures there is also the cost of supplementing with sodium
52
53 99 fumarate and glycerol. The dual aims of this study are to establish whether *E. coli*
54
55 100 cells grown aerobically are capable of manufacturing bioPd and to identify the
56
57
58
59
60

1
2
3 101 enzyme(s) responsible for such metal reduction. A move away from the need for
4
5 102 anaerobic growth would simplify the preparation of high levels of active biomass for
6
7 103 catalyst production at industrial scale.
8
9

10 104

11 105 **Methods**

12 106 *Bacterial growth*

13
14
15
16 107 Starter cultures: 50 ml LB broth in a 500 ml Erlenmeyer flask was inoculated with a
17
18 108 single isolated colony of the *E. coli* strain under investigation and incubated
19
20 109 aerobically (37°C, shaking at 180 rpm for 18 h).
21
22

23 110

24
25 111 Aerobic cultures: An 11 ml starter culture was added to 99 ml LB broth in a 1 L
26
27 112 Erlenmeyer flask. Flasks were incubated for 24 h (37°C, 180 rpm) to produce
28
29 113 stationary phase 'resting' cells. The pH of the cells after 24 h incubation was
30
31 114 measured to determine that organic acids had not been produced that would otherwise
32
33 115 lower the pH considerably (Vasala et al. 2006). Oxygen saturation of a 5 ml aliquot of
34
35 116 the broth culture was measured immediately after 24 h of incubation using an Oakton
36
37 117 D06 Acorn Series dissolved oxygen meter.
38
39

40 118

41 119 *Reduction of Pd(II) to produce bioPd on bacteria*

42
43 120 The aerobically grown liquid culture was divided between two 50 ml Falcon tubes
44
45 121 and washed three times in 20 ml MOPS-NaOH (morpholinepropanesulfonic acid)
46
47 122 buffer, 20 mM at pH7.6 after centrifugation for 20 min at 2500 g. Cell pellets were
48
49 123 adjusted to a mass of 250 mg wet pellet weight, and resuspended in the MOPS-NaOH
50
51 124 buffer to a volume of 1 ml. One tube of 250 mg wet weight cells was resuspended in
52
53 125 22.5 ml MOPS-NaOH buffer with 1 mM sodium tetrachloropalladate in a 30 ml bottle
54
55
56
57
58
59
60

1
2
3 126 sealed with a butyl rubber stopper. The bottle was incubated in the dark at 30°C for 1
4
5 127 h for the Pd(II) to biosorb to the cells (Baxter-Plant et al. 2003). 2.5 ml 10 mM
6
7 128 sodium formate was then added to the bottle to initiate bioreduction of the Pd(II).
8
9

10 129

11
12 130 *Use of mutants to determine electron transfer pathway to Pd(II)*

13
14 131 In order to investigate the possible role of the aerobic formate dehydrogenase (FDH-O)
15
16 132 and other hydrogenase/formate dehydrogenase enzymes in the reduction of Pd(II) by
17
18 133 aerobically-grown cells of *E. coli*, the rates of reduction by six different additional
19
20 134 strains (Table 1) were compared by measuring the Pd(II) remaining in solution by
21
22 135 ICP-MS. The strains were ‘palladised’ as above, and rates of reduction/removal
23
24 136 compared to those in a series of controls: killed cells (MC4100), cell-free suspension,
25
26 137 and live cells (MC4100) unsupplemented with formate.
27
28
29

30 138

31
32 139 All strains except BL21(DE3) were from the culture collection of Professor Frank
33
34 140 Sargent at the College of Life Sciences, University of Dundee. Strain BL21(DE3) was
35
36 141 obtained from Invitrogen, Paisley, UK. Strain MC4100 $\Delta moaA$ was created by
37
38 142 disruption of the *moaA* gene which encodes the molybdenum cofactor biosynthesis
39
40 143 protein A, using the method of Datsenko and Wanner (2000) whereby PCR products
41
42 144 are used to disrupt the gene of choice by recombination using the plasmid-borne
43
44 145 phage λ Red recombinase.
45
46
47

48 146

49
50 147 *X-ray diffraction (XRD) analysis*

51
52 148 The black precipitates were washed once in acetone and air dried, before analysis by
53
54 149 X-ray diffraction (XRD). The measurements were performed on a Bruker D8
55
56 150 Advance diffractometer, using Cu K alpha1 radiation. The samples were scanned
57
58
59
60

1
2
3 151 from 5-70 degrees 2theta in steps of 0.2 degrees, with a count time of 2 seconds per
4
5 152 step.

6
7 153

8
9
10 154 *Extended X-ray absorption fine structure (EXAFS)*

11 155 Aliquots of the cell/Pd/formate suspension were taken at times 0 and 30 min, and 1, 3
12
13
14 156 and 4 h from the addition of formate, and frozen immediately in liquid nitrogen. The
15
16
17 157 direct reduction of Pd(II) to Pd(0) was demonstrated using EXAFS, performed at the
18
19 158 European Synchrotron Radiation Facility (ESRF), in Grenoble, France. The samples
20
21 159 were transported to the synchrotron at ESRF on dry ice, where they were thawed and
22
23 160 injected immediately into sample holders, before freezing once more in liquid
24
25 161 nitrogen and placing into the beam. X-ray absorption data were collected on beamline
26
27 162 BM29 at the Pd K-edge in the energy range 24 200 – 24 900 eV. Data were recorded
28
29 163 at low temperature (77 K) and under vacuum to reduce the thermal Debye-Waller
30
31 164 factor and prevent oxidation. A Si(III) double crystal monochromator was used,
32
33 165 calibrated with a Pd foil, and the spectra were collected in fluorescence mode using a
34
35 166 13-element solid-state detector. A reference spectrum of a palladium foil was
36
37 167 recorded in transmission mode on station 9.3 at the SRS Daresbury. The data were
38
39 168 background subtracted and the EXAFS spectra fitted in DL_Excurv
40
41 169 (<http://www.cse.scitech.ac.uk/cmng/EXCURV/>) using full curved wave theory
42
43 170 (Gurman et al., 1984).

44
45
46
47 171

48
49 172 *Transmission electron microscopy (TEM) and energy dispersive X-ray spectroscopy*
50
51 173 *(EDS)*

52
53
54 174 Following Pd(II) reduction, cells were stored at 10°C overnight. The cell pellets were
55
56 175 then rinsed twice with deionised water, fixed in 2.5% (wt/vol) glutaraldehyde,
57
58
59
60

1
2
3 176 centrifuged for 5 min at 16 000 g, resuspended in 1.5 ml of 0.1 M cacodylate buffer
4
5 177 (pH 7) and stained in 1% osmium tetroxide in 0.1 M phosphate buffer, pH 7 (60 min).
6
7 178 Cells were dehydrated using an ethanol series (70, 90, 100, 100, 100% dried ethanol,
8
9
10 179 15 min each) and washed twice in propylene oxide (15 min, 9500 g). Cells were
11
12 180 embedded in epoxy resin and the mixture was left to polymerise (24 h; 60°C).
13
14 181 Sections (100-150 nm thick) were cut from the resin block, placed onto a copper grid
15
16 182 and viewed with a JEOL 1200CX2 TEM, accelerating voltage 80 keV. EDS was
17
18 183 performed on electron-dark areas, to confirm the presence of palladium.
19
20
21 184

22 23 185 **Results**

24 25 186 *Palladisation of E. coli BL21(DE3)*

26
27 187 The pH of the aerobically-grown liquid culture was between 7.7-7.9, indicating that
28
29 188 there was not extensive production of organic acids due to overflow metabolism.
30
31 189 Oxygen saturation measurements showed that the liquid culture was 72% saturated
32
33 190 following 24 h of incubation, indicating that it was not oxygen-limited. After
34
35 191 harvesting, the cells were able to couple the reduction of Pd(II) to the oxidation of
36
37 192 formate, indicated by the rapid formation of a black precipitate, tentatively identified
38
39 193 as Pd(0) (Figure 1). ICP-MS analysis confirmed complete removal of Pd(II) from
40
41 194 solution within 45 min, and the presence of crystalline Pd(0) was confirmed using
42
43 195 XRD in this, but not in the heat-killed cells control where the cells removed
44
45 196 substantial Pd(II) abiotically. An increase in metal biosorption by heat killed biomass
46
47 197 as compared to live cells is well documented (Machado et al. 2009; Parameswari et al.
48
49 198 2009) and was attributed to loss of membrane integrity to reveal additional
50
51 199 intracellular metal binding sites (Machado et al. 2009).
52
53
54
55
56
57
58
59
60

1
2
3 201 *Extended X-ray absorption fine structure (EXAFS)*
4

5 202 The nature of the Pd associated with the biomass was assessed further using X-ray
6
7 203 absorbance spectroscopy. The features in the corresponding EXAFS spectra (Figure 2)
8
9 204 are due to the wave-like nature of the photoelectron, which is released from the atom
10
11 205 with increasing energy and scattered from surrounding atoms with new waves being
12
13 206 emitted. With increasing photon energy, the interference between the waves alternates
14
15 207 between constructive and destructive, which leads to oscillations in the spectrum.
16
17 208 Examining these oscillations gives information on the number, species and distance of
18
19 209 the surrounding atoms. As seen in Figure 2, the samples taken at times 0 and 30 min,
20
21 210 which contain Pd(II), have identical EXAFS spectra. The samples taken at 60 min
22
23 211 onwards are identical to the Pd(0) foil control, which indicates that only Pd(0) was
24
25 212 present. Reduction of the Pd(II) to Pd(0) was therefore confirmed to be complete in
26
27 213 less than 30 min, as confirmed by ICP-MS analysis.
28
29
30
31

32 214

33
34 215 *Use of mutants to determine electron transfer pathway to Pd(II)*
35

36 216 Aerobic cultures of the parental strains MC4100 and BW25113 and the strain which
37
38 217 lacked all hydrogenases (JW2682) removed Pd(II) identically with no residual Pd(II)
39
40 218 detected after 30 min (Figure 3). Removal of the hydrogenase enzymes had no effect
41
42 219 on the rate of palladium removal from solution, confirming that these hydrogenases
43
44 220 have no role in the aerobic reduction of Pd(II). The FDH-O-negative strain JW3865
45
46 221 reduced Pd(II) within 1 h, and the FDH-O/FDH-N-negative strain FTD128 within 2 h.
47
48 222 Strain MC4100 $\Delta moaA$, lacking all molybdoenzymes, reduced the palladium within 7
49
50 223 h. These results indicate the likely involvement of the FDH-O enzyme in the
51
52 224 reduction of Pd(II) by aerobically-grown *E. coli* using formate, although other Mo-
53
54 225 containing enzymes must also be involved given the impaired metal reduction noted
55
56
57
58
59
60

1
2
3 226 with the Δmoa mutant. Controls containing no biomass showed no abiotic reduction
4
5 227 of Pd(II) using formate (Figure 1B), although a brown precipitate was seen in the no-
6
7 228 formate control. The X-ray powder diffraction pattern did not show the presence of
8
9 229 any peaks characteristic of Pd(0) in this precipitate, indicating that it was probably
10
11 230 amorphous and non-crystalline. Time zero on Figure 3 is the point at which formate
12
13 231 was added, following 1 h of incubation to allow biosorption of the Pd(II) to the cells;
14
15 232 hence the abiotic Pd(II) removal by killed cells (Figure 1) was apparent at the time of
16
17 233 formate addition with no evidence for further Pd(II) reduction.
18
19
20
21 234

22 235 *Transmission electron microscopy (TEM)*

23 236 TEM images of thin sections of cells showed that with all strains the reduced
24
25 237 palladium was precipitated predominantly in the extracellular matrix of the cultures
26
27 238 (Figure 4), although it appears that the nanoparticles may be associated with the outer
28
29 239 membrane of the cells. Energy dispersive X-ray spectroscopy (EDS) confirmed the
30
31 240 presence of palladium in these precipitates.
32
33
34
35 241

36 242 **Discussion**

37
38 243 The results from this study demonstrate that it is possible for aerobically-grown
39
40 244 cultures of *E. coli* to reduce Pd(II) enzymatically, with no need to remove oxygen
41
42 245 from the experimental system during the bioreduction step. Autoclaved control
43
44 246 experiments indicate that Pd(II) bioreduction in these cultures is enzymatic, with
45
46 247 reduction of palladium not occurring in the absence of viable cells irrespective of the
47
48 248 length of incubation. The major enzymes shown to be involved include the formate
49
50 249 dehydrogenases FDH-O and FDH-N, although bioreduction still occurs in strains
51
52 250 without these enzymes albeit at a much lower rate. Other molybdoenzymes must
53
54
55
56
57
58
59
60

1
2
3 251 therefore be involved. The strain that lacked all molybdoenzymes did however still
4
5 252 reduce the palladium, although this took 7 h, compared with less than 30 min by the
6
7 253 wild-type strains. Hydrogenases, implicated as the dominant Pd(II) reductases in other
8
9
10 254 experimental systems grown under anaerobic conditions (Deplanche et al. 2010;
11
12 255 Mikheenko et al. 2008), are not expressed in aerobically grown cultures, and their
13
14 256 lack of involvement was evident as the strain lacking hydrogenase enzymes reduced
15
16 257 palladium at the same rate as the wild-type strains in this study.
17
18
19 258

20
21 259 Furthermore, whichever biological system is responsible for the aerobic bioreduction
22
23 260 of Pd(II), there seems to be little impact on the site of Pd(0) deposition. The location
24
25 261 of the bioreduced Pd(0) in our experiments is almost always extracellular, although
26
27 262 often associated with the outer membrane of the cells. This is particularly the case
28
29
30 263 with the MC4100 $\Delta moaA$ strain (which lacks all molybdoenzymes), in which the
31
32 264 majority of the Pd(0) nanoparticles are closely associated with the outer membrane
33
34 265 (Figure 4E). One conclusion that may be drawn from this is that whilst cells that lack
35
36 266 the formate dehydrogenases are still capable of reducing Pd(II), when all of these
37
38 267 enzymes are missing a cellular component associated with the outer membrane may
39
40 268 be responsible. Furthermore, this formate oxidation activity is much weaker than that
41
42
43 269 seen with the strains containing formate dehydrogenases, where Pd(II) reduction is
44
45 270 more rapid. It is possible however that following the initial enzymatic reduction of a
46
47 271 small percentage of the Pd(II), the Pd(0) nanoparticles formed may themselves be
48
49
50 272 responsible for catalysing the reduction of the remainder of the Pd(II) (Yong et al.
51
52 273 2002), which would mean that only a minor, initial biological input is required.
53
54 274

1
2
3 275 Although the formate dehydrogenase enzyme systems implicated in Pd(II)
4
5 276 bioreduction by *E. coli* are periplasmic, the majority of the reduced Pd(0) precipitates
6
7 277 outside the cell. It is possible that an electron shuttle system exists similar to that
8
9 278 found in *Shewanella oneidensis* (von Canstein et al. 2008) that is as yet undiscovered
10
11 279 in *E. coli*. It is also possible that the first Pd(0) nanoparticles to form breach the outer
12
13 280 membrane, and themselves form an electron conduit for further Pd(II) reduction
14
15 281 outside the cell. The pH of these experiments is also higher than others where Pd(0)
16
17 282 nanoparticles accumulated in the periplasm (Redwood et al. 2008), which could
18
19 283 indicate the higher biosorption of cationic metal to the outer membrane and
20
21 284 extracellular polymeric substances, which are then not able to enter the periplasm.
22
23 285 The influence of a higher pH in the location of the Pd(0) may be confirmed by the
24
25 286 observation that Pd(0) nanoparticles were located on the cell surface of *D.*
26
27 287 *desulfuricans* when bioreduction of Pd(II) was performed at pH 7 (Yong et al. 2002).
28
29 288
30
31
32
33
34 289 In conclusion, this study has demonstrated the presence of a novel biological
35
36 290 mechanism responsible for the bioreduction of Pd(II) in aerobically-grown cultures of
37
38 291 *E. coli*, catalysed mainly by molybdenum-containing enzyme systems. Subsequent
39
40 292 studies will investigate the catalytic activity and selectivity of the Pd(0) nanoparticles
41
42 293 produced under aerobic conditions in a range of industrially important reactions. If
43
44 294 active, this new form of bioPd has the advantage over that produced by anaerobic
45
46 295 culture as it is easier to produce at high yield, from increased biomass levels
47
48 296 associated with aerobic growth. There is also no requirement for additional processing
49
50 297 steps to remove H₂S (produced by SRB systems), and the use of formate instead of
51
52 298 hydrogen gas means that the procedure is less hazardous and more controllable. The
53
54 299 advantages of this more scalable method of synthesis would need to be considered
55
56
57
58
59
60

1
2
3 300 against any alterations in activity/selectivity of the resulting catalyst (versus synthetic
4
5 301 and other bioPds), using a cost-benefit analysis. Importantly, identification of the
6
7 302 specific enzymatic process(es) involved in the biomanufacture of bioPd is the first
8
9
10 303 step towards application of the tools of synthetic biology for ‘designer catalyst’
11
12 304 production for specific applications.

13 305
14
15
16 306 In a geomicrobiological context, this study shows that aerobic cells of *E. coli* restrict
17
18 307 the deposition of Pd(0) to locations outside the cell. However in both *D. desulfuricans*
19
20 308 (grown anaerobically) and *Bacillus benzovorans* (grown aerobically) intracellular
21
22 309 depositions of small Pd-nanoparticles were observed at the expense of both hydrogen
23
24 310 and formate (JB Omajali, IP Mikheenko, ML Merroun, J Wood and LE Macaskie, in
25
26 311 press) and, notably, were also seen in *E. coli* grown anaerobically (LE Macaskie, A
27
28 312 Williams, R Priestley and J Courtney, unpublished). This raises questions about
29
30 313 potential biochemical ‘trafficking’ pathways of Pd(II), the possibility of Pd(II) efflux
31
32 314 by aerobic (but not anaerobic) cells and, following from that, the possibility of
33
34 315 biogeochemical cycling of this element.
35
36
37
38
39

316

317 **Acknowledgement**

318 The authors would like to thank Dr Victoria Coker, Prof Richard Pattrick, and Dr
319 John Charnock of the University of Manchester for assistance with EXAFS.

320

321 **Funding**

322 This study was supported by a grant from the Biotechnology and Biological Sciences
323 Research Council (BBSRC).

324

325 **References**

- 326 Abaibou H, Pommier J, Benoit S, Giordano G, Mandrandberthelot MA. 1995.
327 Expression and characterization of the *Escherichia coli fdo* Locus and a possible
328 physiological role for aerobic formate dehydrogenase. Journal of Bacteriology
329 177:7141-7149.
330
331 Baba T, Ara T, Hasegawa M, Takai Y, Okumura Y, Baba M, Datsenko KA, Tomita
332 M, Wanner BL, Mori H. 2006. Construction of *Escherichia coli* K-12 in-frame,
333 single-gene knockout mutants: the Keio collection. Molecular Systems Biology 2:
334 Article no. 2006.0008.
335
336 Baxter-Plant V, Mikheenko IP, Macaskie LE. 2003. Sulphate-reducing bacteria,
337 palladium and the reductive dehalogenation of chlorinated aromatic compounds.
338 Biodegradation 14:83-90.
339
340 Beauregard D, Yong P, Macaskie LE, Johns ML. 2010. Using non-invasive magnetic
341 resonance imaging (MRI) to assess the reduction of Cr(VI) using a biofilm-palladium
342 catalyst. Biotechnology and Bioengineering 107:11-20.
343
344 Bennett JA, Creamer NJ, Deplanche K, Macaskie LE, Shannon IJ, Wood J. 2010.
345 Palladium supported on bacterial biomass as a novel heterogeneous catalyst: A
346 comparison of Pd/Al₂O₃ and bio-Pd in the hydrogenation of 2-pentyne. Chemical
347 Engineering Science 65:282-290.
348

- 1
2
3 349 Bennett JA, Mikheenko I, Deplanche K, Shannon IJ, Wood J. & Macaskie LE. 2013.
4
5 350 Nanoparticles of palladium supported on bacterial biomass: new re-usable
6
7 351 heterogeneous catalyst with comparable catalytic activity to homogeneous colloidal
8
9 352 palladium in the Heck reaction. *Applied Catalysis B Environmental* 140-141:700-707.
10
11 353
12
13 354 Bunge M, Søbberg LS, Rotaru AE, Gauthier D, Lindhardt AT, Hause G, Finster K,
14
15 355 Kingshott P, Skrydstrup T, Meyer RL. 2010. Formation of palladium (0)
16
17 356 nanoparticles at microbial surfaces. *Biotechnology and Bioengineering* 107:206-215.
18
19 357
20
21 358 Casadaban MJ, Cohen SN. 1979. Lactose genes fused to exogenous promoters in one-
22
23 359 step using a *Mu-lac* Bacteriophage: *in vivo* probe for transcriptional control sequences.
24
25 360 *Proceedings of the National Academy of Sciences of the United States of*
26
27 361 *America* 76:4530-4533.
28
29 362
30
31 363 Chidambaram D, Hennebel T, Taghavi S, Mast J, Boon N, Verstraete W, van der
32
33 364 Lelie D, Fitts JP. 2010. Concomitant microbial generation of palladium nanoparticles
34
35 365 and hydrogen to immobilize chromate. *Environmental Science & Technology*
36
37 366 44:7635-7640.
38
39 367
40
41 368 Creamer NJ, Mikheenko IP, Yong P, Deplanche K, Sanyahumbia D, Wood J,
42
43 369 Pollmann K, Merroun M, Selenska-Pobell S, Macaskie LE. 2007. Novel supported Pd
44
45 370 hydrogenation bionanocatalyst for hybrid homogeneous/heterogeneous catalysis.
46
47 371 *Catalysis Today* 128:80-87.
48
49 372
50
51
52
53
54
55
56
57
58
59
60

- 1
2
3 373 Datsenko KA, Wanner BL. 2000. One-step inactivation of chromosomal genes in
4
5 374 *Escherichia coli* K-12 using PCR products. Proceedings of the National Academy of
6
7 375 Sciences of the United States of America 97:6640-6645.
8
9 376
10
11 377 De Windt W, Aelterman P, Verstraete, W. 2005. Bioreductive deposition of palladium
12
13 378 (0) nanoparticles on *Shewanella oneidensis* with catalytic activity towards reductive
14
15 379 dechlorination of polychlorinated biphenyls. Environmental Microbiology 7:314-325.
16
17 380
18
19 381 Deplanche K, Caldelari I, Mikheenko IP, Sargent F, Macaskie LE. 2010. Involvement
20
21 382 of hydrogenases in the formation of highly catalytic Pd(0) nanoparticles by
22
23 383 bioreduction of Pd(II) using *Escherichia coli* mutant strains. Microbiology 156:2630-
24
25 384 2640.
26
27 385
28
29 386 Deplanche K, Bennett JA, Mikheenko IP, Omajali J, Wells AS, Meadows PE, Wood J,
30
31 387 Macaskie LE. 2014. Catalytic activity of biomass supported palladium nanoparticles:
32
33 388 influence of the biological component in catalytic efficacy and potential applications
34
35 389 in green synthesis of fine chemicals and pharmaceuticals. Applied Catalysis B
36
37 390 Environmental 147:651-665.
38
39 391
40
41 392 Gauthier D, Søbjerg LS, Jensen KM, Lindhardt AT, Bunge M, Finster K, Skrydstrup
42
43 393 T, Meyer RL. 2010. Environmentally benign recovery and reactivation of palladium
44
45 394 from industrial waste by using Gram-negative bacteria. Chemsuschem 3:1036-1039.
46
47 395
48
49 396 Gurman SJ, Binsted N, Ross I. 1984. A rapid, exact curved-wave theory for EXAFS
50
51 397 calculations. Journal of Physics C: Solid State Physics 17:143-151.
52
53
54
55
56
57
58
59
60

1
2
3 398
4
5 399 Harrad S, Robson M, Hazrati S, Baxter-Plant VS, Deplanche K, Redwood MD,
6
7 400 Macaskie LE. 2007. Dehalogenation of polychlorinated biphenyls and
8
9 401 polybrominated diphenyl ethers using a hybrid bioinorganic catalyst. Journal of
10
11 402 Environmental Monitoring 9:314-318.
12
13 403
14
15
16 404 Hennebel T, Verhagen P, Simoen H, De Gusseme B, Vlaeminck SE, Boon N,
17
18 405 Verstraete W. 2009a. Remediation of trichloroethylene by bio-precipitated and
19
20 406 encapsulated palladium nanoparticles in a fixed bed reactor. Chemosphere 76:1221-
21
22 407 1225.
23
24 408
25
26
27 409 Hennebel T, Simoen H, De Windt W, Verloo M, Boon N, Verstraete W. 2009b.
28
29 410 Biocatalytic dechlorination of trichloroethylene with bio-palladium in a pilot-scale
30
31 411 membrane reactor. Biotechnology and Bioengineering 102:995-1002.
32
33 412
34
35
36 413 Lloyd JR. 2003. Microbial reduction of metals and radionuclides. FEMS
37
38 414 Microbiology Reviews 27:411-425.
39
40 415
41
42
43 416 Lloyd JR, Pearce CI, Coker VS, Patrick RA, van der Laan G, Cutting R, Vaughan DJ,
44
45 417 Paterson-Beedle M, Mikheenko IP, Yong P, Macaskie LE. 2008. Biomineralization:
46
47 418 linking the fossil record to the production of high value functional materials.
48
49 419 Geobiology 6:285-297.
50
51 420
52
53
54 421 Lovley DR. 2006. Microbial fuel cells: novel microbial physiologies and engineering
55
56 422 approaches. Current Opinion in Biotechnology 17:327-332.
57
58
59
60

- 1
2
3 423
4
5 424 Luke I, Butland G, Moore K, Buchanan G, Lyall V, Fairhurst SA, Greenblatt JF,
6
7 425 Emili A, Palmer T, Sargent F. 2008. Biosynthesis of the respiratory formate
8
9 426 dehydrogenases from *Escherichia coli*: characterization of the FdhE protein. Archives
10
11 427 of Microbiology 190:685-696.
12
13 428
14
15 429 Mabbett A, Sanyahumbi D, Yong P, Macaskie LE. 2006. Biorecovered precious
16
17 430 metals from industrial wastes: Single-step conversion of a mixed metal liquid waste to
18
19 431 a bioinorganic catalyst with environmental application. Environmental Science &
20
21 432 Technology 40:1015-1021.
22
23 433
24
25 434 Machado MD, Janssens S, Soares HMVM, Soares EV. 2009. Removal of heavy
26
27 435 metals using a brewers' yeast strain of *Saccharomyces cerevisiae*: advantages of using
28
29 436 dead biomass. Journal of Applied Microbiology 106:1792-1804.
30
31 437
32
33 438 Mertens B, Blothe C, Windey K, De Windt W, Verstraete W. 2007. Biocatalytic
34
35 439 dechlorination of lindane by nano-scale particles of Pd(0) deposited on *Shewanella*
36
37 440 *oneidensis*. Chemosphere 66:99-105.
38
39 441
40
41 442 Mikheenko IP, Rousset M, Dementin S, Macaskie LE. 2008. Bioaccumulation of
42
43 443 palladium by *Desulfovibrio fructosivorans* wild-type and hydrogenase-deficient
44
45 444 strains. Applied and Environmental Microbiology 74:6144-6146.
46
47 445
48
49 446 Orozco RL, Redwood MD, Yong P, Macaskie LE. 2010. Towards an integrated
50
51 447 system for bio-energy: hydrogen production by *Escherichia coli* and use of
52
53
54
55
56
57
58
59
60

- 1
2
3 448 palladium-coated waste cells for electricity generation in a fuel cell. *Biotechnology*
4
5 449 *Letters* 32:1837-1845.
6
7 450
8
9 451 Paramewsari E, Lakshmanan A, Thilagavathi T. 2009. Effect of pretreatment of blue
10
11 452 green algal biomass on biosorption of chromium and nickel. *Journal of Algal Biomass*
12
13 453 *Utilisation* 1:9-17.
14
15 454
16
17 455 Redwood MD, Deplanche K, Baxter-Plant VS, Macaskie LE. 2008. Biomass-
18
19 456 supported palladium catalysts on *Desulfovibrio desulfuricans* and *Rhodobacter*
20
21 457 *sphaeroides*. *Biotechnology and Bioengineering* 99:1045-1054.
22
23 458
24
25 459 Søjberg LS, Gauthier D, Lindhardt AT, Bunge M, Finster K, Skrydstrup T, Meyer RL.
26
27 460 2009. Bio-supported palladium nanoparticles as a catalyst for Suzuki-Miyaura and
28
29 461 Mizoroki-Heck reactions. *Green Chemistry* 11:2041-2046.
30
31 462
32
33 463 Studier FW, Moffatt BA. 1986. Use of bacteriophage T7 RNA polymerase to direct
34
35 464 selective high level expression of cloned genes. *Journal of Molecular Biology*
36
37 465 189:113-130.
38
39 466
40
41 467 Vasala A, Panula J, Bollok M, Illmann L, Halsig C, Neubauer P. 2006. A new
42
43 468 wireless system for decentralised measurement of physiological parameters from
44
45 469 shake flasks. *Microbial Cell Factories* 5:8.
46
47 470
48
49
50
51
52
53
54
55
56
57
58
59
60

- 1
2
3 471 von Canstein H, Ogawa J, Shimizu S, Lloyd JR. 2008. Secretion of flavins by
4
5 472 *Shewanella* species and their role in extracellular electron transfer. Applied and
6
7 473 Environmental Microbiology 74:615-623.
8
9 474
10
11 475 Wood J, Bodenes L, Bennett J, Deplanche K, Macaskie LE. 2010. Hydrogenation of
12
13 476 2-butyne-1,4-diol using novel bio-palladium catalysts. Industrial & Engineering
14
15 477 Chemistry Research 49:980-988.
16
17 478
18
19
20 479 Yong P, Rowson N., Farr JPG, Harris IR, Macaskie, LE. 2002. Bioreduction and
21
22 480 biocrystallization of palladium by *Desulfovibrio desulfuricans* NCIMB 8307.
23
24 481 Biotechnology and Bioengineering 80:369-379.
25
26 482
27
28
29 483 Yong P, Paterson-Beedle M, Mikheenko IP, Macaskie LE. 2007. From bio-
30
31 484 mineralisation to fuel cells: biomanufacture of Pt and Pd nanocrystals for fuel cell
32
33 485 electrode catalyst. Biotechnology Letters 29:539-544.
34
35 486
36
37 487
38
39 488
40
41 489
42
43 490
44
45 491
46
47 492
48
49 493
50
51 494
52
53
54
55
56
57
58
59
60

495 **Table 1.** *E. coli* strains used to determine biological involvement in the reduction of
 496 palladium (II) using formate as the electron donor.

Strain	Genotype	Phenotype	Reference
BL21(DE3)	<i>F2 ompT gal dcm lon hsdS_B(r_B⁻ m_B⁻) λ(DE3 [lacI lacUV5-T7 gene 1 ind1 sam7 nin5])</i>	Wild type strain commonly used for recombinant protein expression.	(Studier and Moffatt 1986)
MC4100	<i>F- ΔlacU169 araD139 rpsL150 relA1 ptsF rbs flbB5301</i>	Parental strain for FTD128 and $\Delta moaA$.	(Casadaban and Cohen 1979)
BW25113	<i>lacI^f rrbB_{T14} ΔlacZ_{WJ16} hsdR514 ΔaraBAD_{AH33} ΔrhaBAD_{LD78}</i>	Parental strain for JW2682 and JW3865.	(Datsenko and Wanner 2000)
FTD128	As MC4100, with in-frame deletion in the <i>fdhE</i> gene.	FDH-O & FDH-N negative.	(Luke et al. 2008)
JW2682	As BW25113, with in-frame deletion of the <i>hypF</i> gene.	Deficient in all hydrogenases.	(Baba et al. 2006)
JW3865	As BW25113, with in-frame deletion of the <i>fdoG</i> gene.	FDH-O negative.	(Baba et al. 2006)
MC4100 $\Delta moaA$	As MC4100, disruption of the <i>moaA</i> gene.	Deficient in all molybdoenzymes	This study.

497

498

499

500

501

502

1
2
3
4
5
6
7
8
9
10
11
12
13
14
15
16
17
18
19
20
21
22
23
24
25
26
27
28
29
30
31
32
33
34
35
36
37
38
39
40
41
42
43
44
45
46
47
48
49
50
51
52
53
54
55
56
57
58
59
60

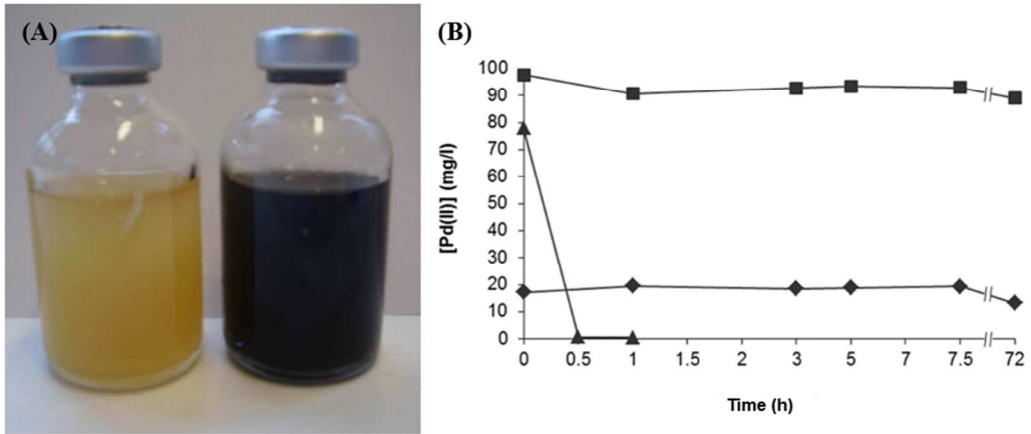
503 **Fig. 1.** (A) Complete reduction of Pd(II) to Pd(0) by an aerobically-grown culture of
504 *E. coli*. Both bottles contain cells resuspended in 20 mM MOPS buffer at pH7.6, and
505 1 mM sodium tetrachloropalladate (total volume 25 ml). This image was taken 45 min
506 after the addition of formate to the bottle on the right. (B) Reduction by *E. coli*
507 MC4100 and by controls showing no abiotic reduction of Pd(II). Controls used were
508 killed (autoclaved) cells and cell-free suspension. Soluble Pd(II) in the supernatant
509 was measured using ICP-MS. ▲ = MC4100; ■ = no cells; ◆ = killed cells.

510
511 **Fig. 2.** EXAFS data showing the presence of Pd(II) at 0 and 30 min (bottom two
512 traces), and Pd(0) at 1, 3 and 4 h (ascending series). The top trace is palladium foil.

513
514 **Fig. 3.** Pd(II) reduction by six different strains of *E. coli*, using formate as the electron
515 donor. Soluble Pd(II) in the supernatant was measured using ICP-MS. ◆ = BW25113;
516 □ = JW2682; ▲ = JW3865; Δ = MC4100 $\Delta moaA$; ■ = MC4100; ◇ = FTD128. Data
517 points for BW25113, JW2682 and JW3865 are mean values of triplicates, with
518 standard error shown.

519
520 **Fig. 4.** TEM of thin sections of aerobically grown cells showing extracellular
521 palladium; (A) MC4100, inset BL21; (B) BW25113, inset BL21 (no Pd); (C)
522 FTD128; (D) JW2682; (E) MC4100 $\Delta moaA$; (F) JW3865. Scale bar (A) = 100 nm;
523 (B)-(F) = 500 nm; insets = 1 μ m.

528 **Figure 1**

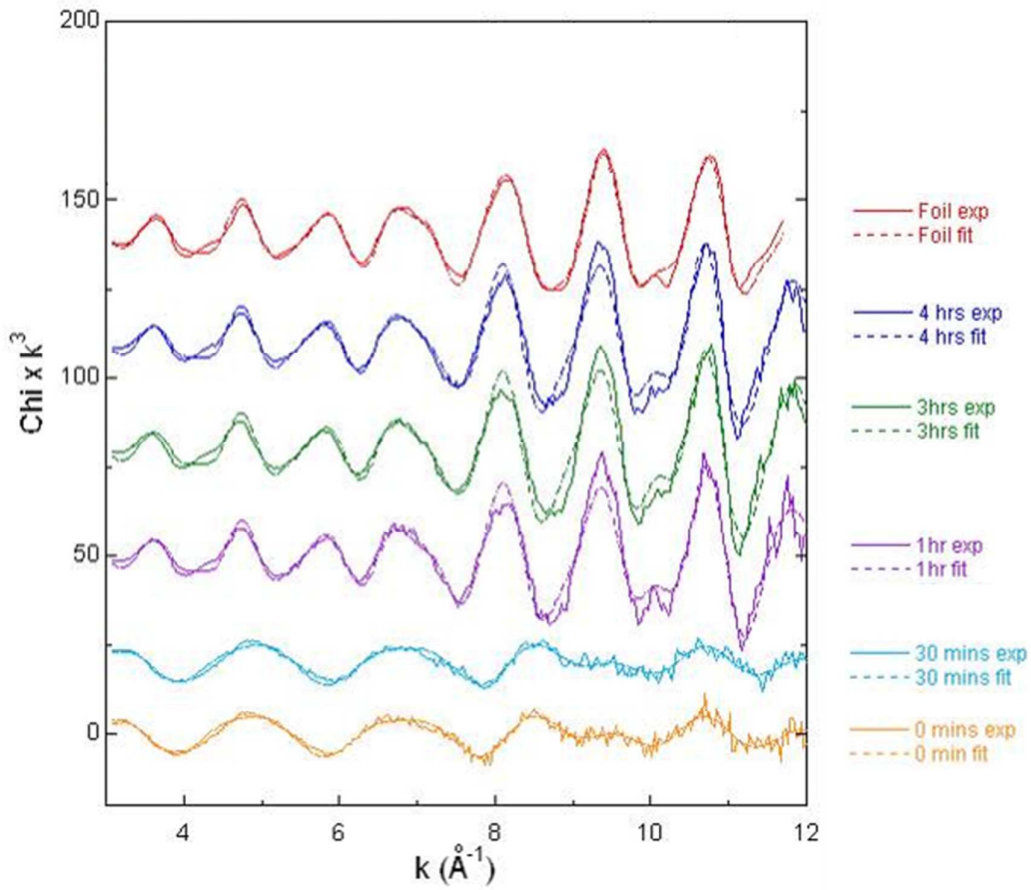


529

530

531

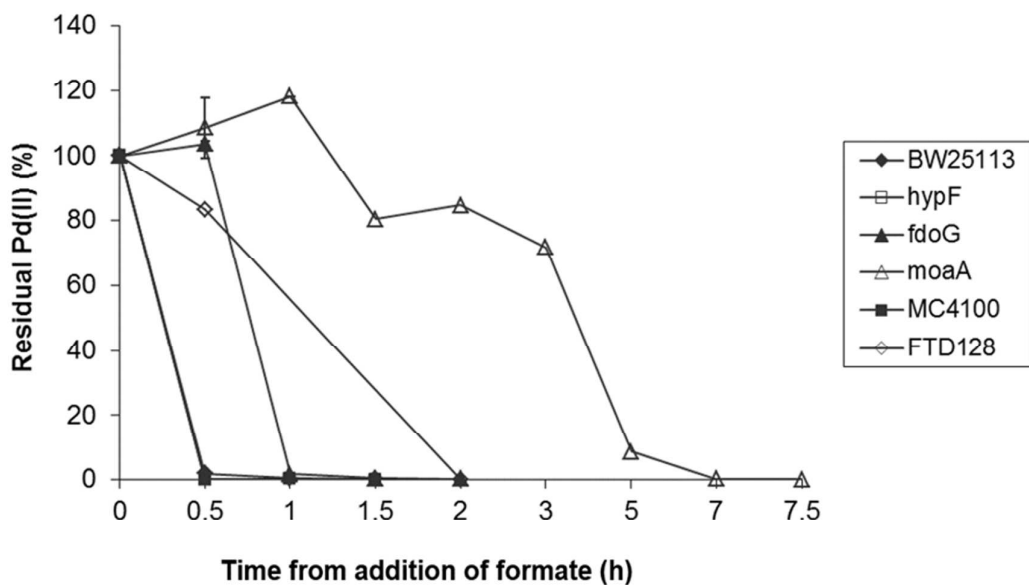
532 **Figure 2**



533

534

535 **Figure 3**



536

537

538

539

540

541

542

543

544

545

546

547

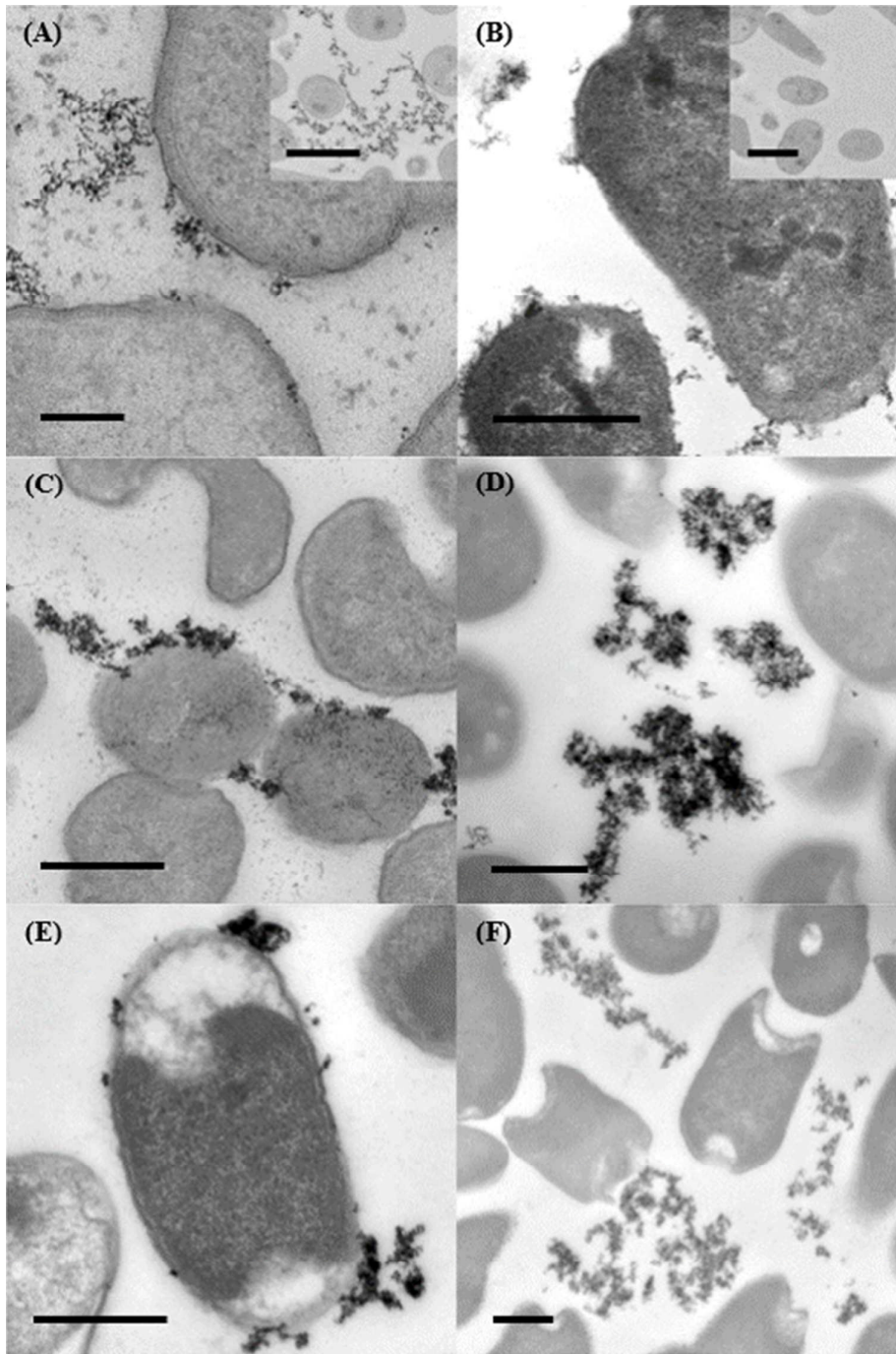
548

549

550

551

552 Figure 4



553

554